Supporting Information

Franzenburg et al. 10.1073/pnas.1304960110

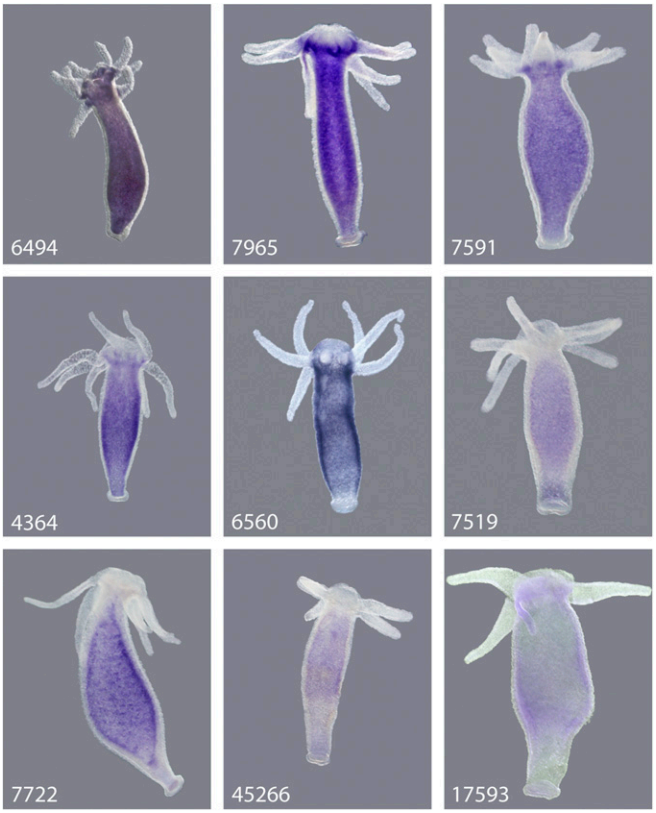

Fig. S1. In situ hybridization localizes most arminins in endodermal epithelial cells. Expression of nine *arminin* paralogs in *Hydra vulgaris* (AEP), localized by whole-mount in situ hybridization. Blue staining indicates endogenous arminin transcripts. Except *arminin6560,* all candidates are localized in the endoderm. Numbers at the lower left hand corner of each picture indicate the contig number of the *arminin* candidate gene. Magnification: 100×.

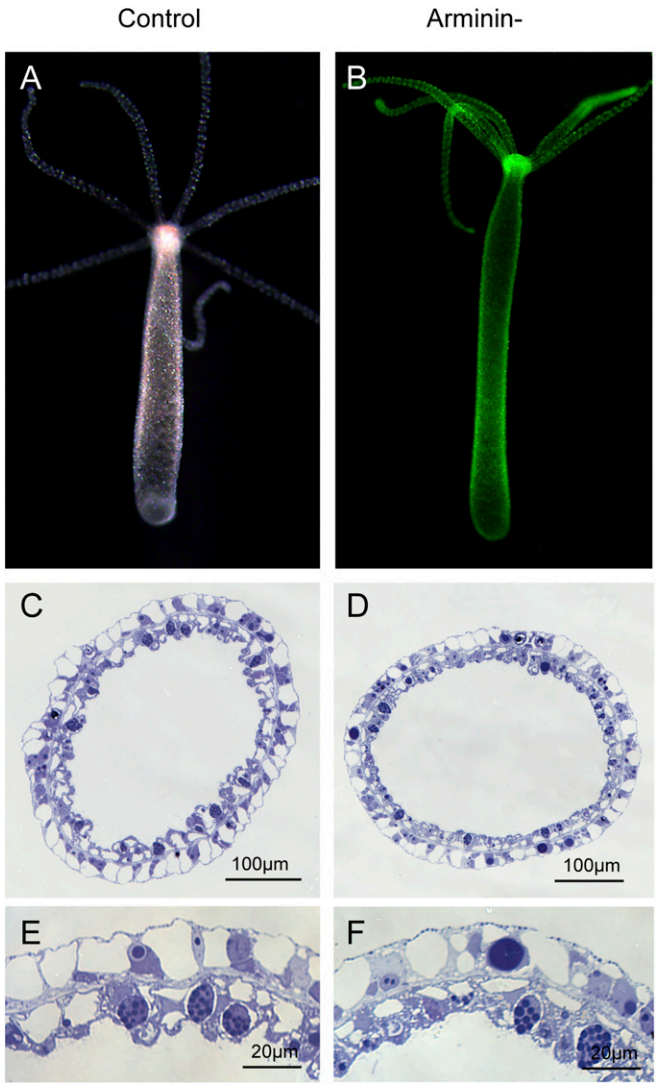

Fig. S2. Images of whole-mount and sectioned Arminin^{-} and control polyps. (*A*) Control polyps. Magnification: 50×. (*B*) Transgenic polyp carrying the transgene in endodermal epithelial cells (actin::eGFP:Arminin-hairpin). Magnification: 50×. (*C* and *E*) Histology (stained with Richardson) of cross-sections of control polyps. (*D* and *F*) Histology of cross sections of Arminin^{-} polyps.

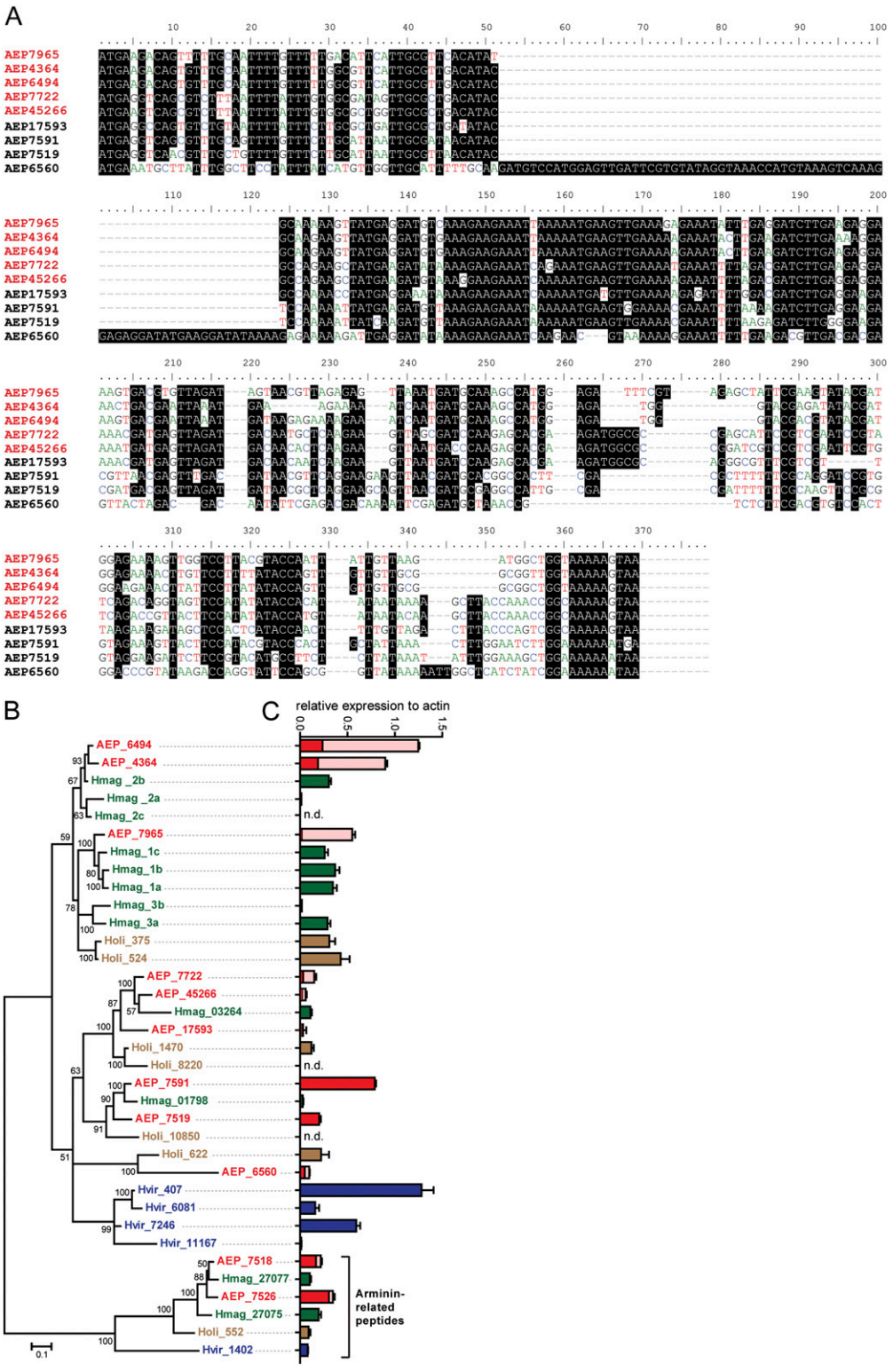

Fig. S3. Arminin knockdown shifts the profile of arminin expression. (*A*) Clustal W alignment of the coding sequence of *H. vulgaris* (AEP) arminins. Nucleotides with ≥ 75% identity in all paralogs are shaded black. The complete coding sequence of *arminin7965* was used to generate the hairpin construct. Note the relatively conserved region between base 130 and 200. Red sequences: all genes which were significantly down-regulated because of the overexpression of the hairpin cassette containing the *arminin*7965 antisense and sense sequences. (*B*) Phylogenetic analysis of the arminin AMP family from four different *Hydra* species. The tree was built by Bayesian interference of phylogeny. Posterior probabilities are shown at the corresponding nodes. Relative expression of each *arminin*, compared with the expression of *β-actin* from the corresponding species. Expression data were retrieved from microarray data. Light red represents original expression (compare Fig. 3), dark red represents remaining expression after *arminin* knockdown, calculated with fold-changes retrieved by quantitative real-time PCR (qRT-PCR).

Fig. S4. Generation of germ-free control and Arminin^{-} polyps. Absence of bacteria after antibiotic treatment was confirmed by PCR amplification of the bacterial 16S rRNA gene using eubacterial specific primers Eub-27F and Eub-1492R (1) in a 30-cycle PCR. Nongerm-free *H. vulgaris* (AEP) wild-type polyps were included as positive control. NTC, nontemplate control. Template DNAs were equilibrated using β-*actin*.

1. Weisburg WG, Barns SM, Pelletier DA, Lane DJ (1991) 16S ribosomal DNA amplification for phylogenetic study. *J Bacteriol* 173(2):697–703.

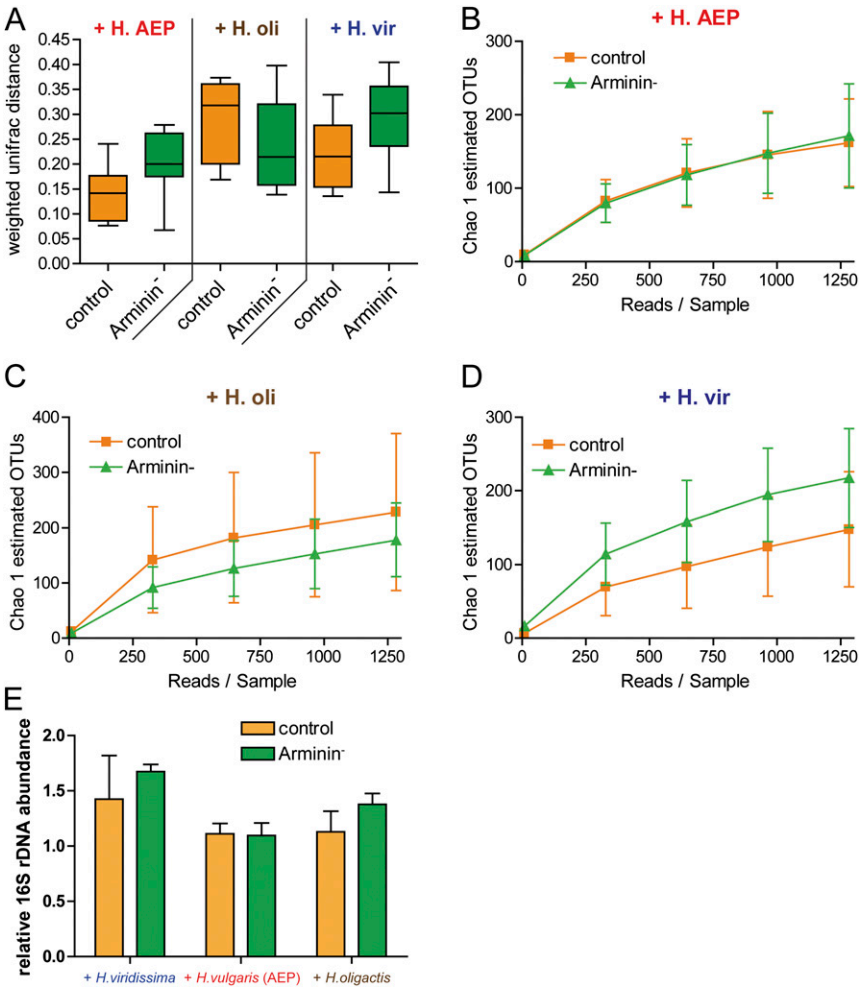

Fig. S5. Comparison of the interindividual microbiota variation, bacterial species diversity and bacterial load. (*A*) Comparison of weighted Unifrac distances within treatments shows no significant differences in the variability of the microbiota composition between control and Arminin^{-} polyps. Statistics were carried out using one way ANOVA with Bonferroni correction: $*P < 0.05$, $**P < 0.01$, $***P < 0.001$. (*B–D*) Chao 1 estimated α-diversities. No significant differences in microbiota diversity were observed between control and Arminin^{-} samples (two-tailed *t* test: $*P < 0.05$, $**P < 0.01$, $***P < 0.001$). (*E*) qPCR quantification of bacterial load of exgerm-free control and Arminin^{-} polyps after inoculation with bacterial communities by cocultivation with different *Hydra* species. qRT-PCR was conducted with the primers Eub341_F and Eub534_R (1), equilibrated to the β-*actin* gene. Error bars represent SEM. Statistical analysis was conducted by two-tailed *t* test, but no significant differences were observed; $n = 5$.

1. Muyzer G, de Waal EC, Uitterlinden AG (1993) Profiling of complex microbial populations by denaturing gradient gel electrophoresis analysis of polymerase chain reaction-amplified genes coding for 16S rRNA. *Appl Environ Microbiol* 59(3):695–700.

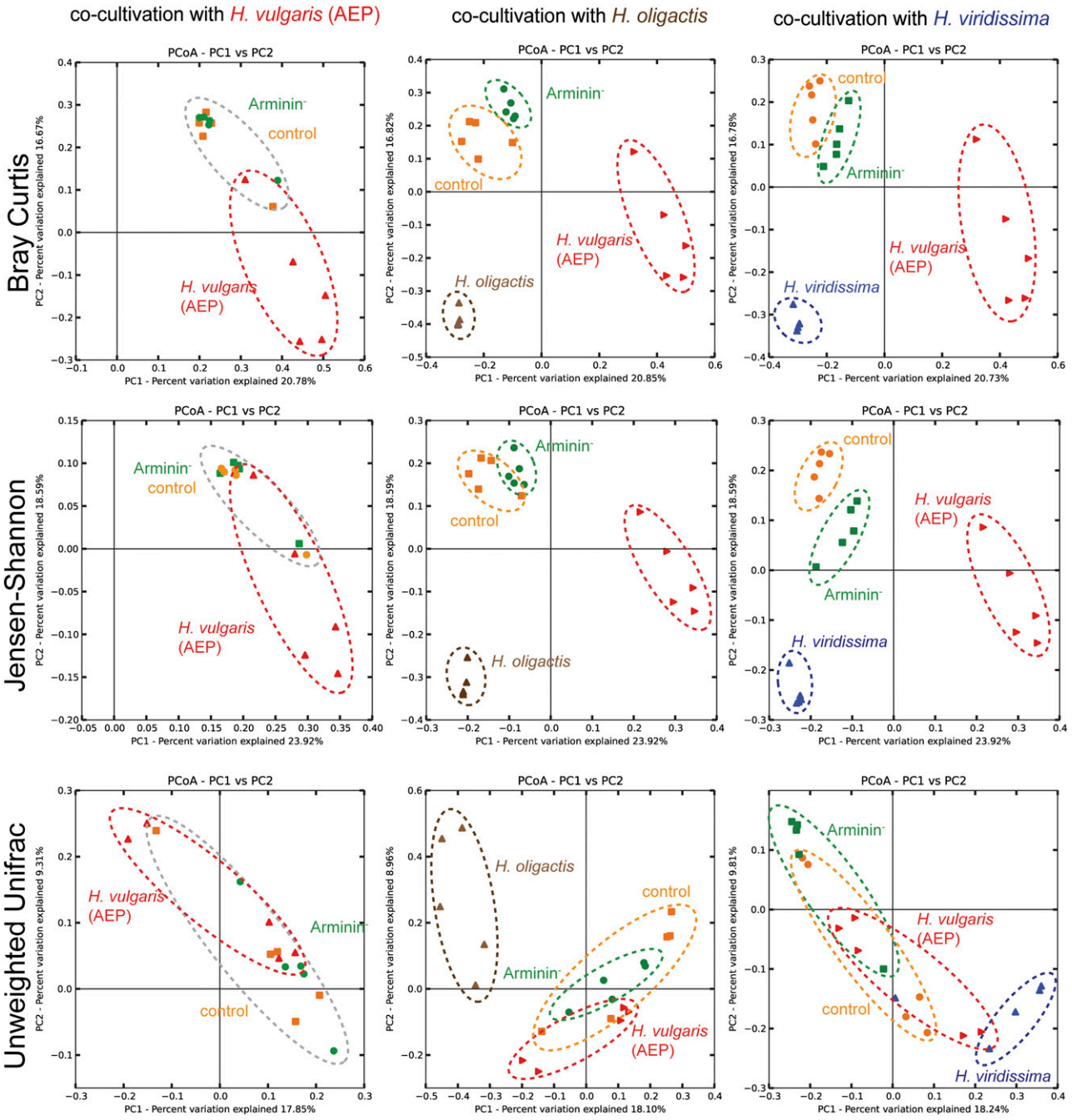

Fig. S6. Bacterial communities were evaluated by principle coordinate analysis (PCoA) based on Bray–Curtis, Jensen–Shannon, and unweighted Unifrac distances. (*Left*) Inoculated with native bacteria retrieved from *H. vulgaris* (AEP); (*Center*) Cocultivated with *Hydra Oligactis*; (*Right*) Cocultivated with *Hydra viridissima*. All three PCoA plots of one metric are based on the same distance matrix containing all 45 samples and, therefore, all samples are presented relative to each other. The percent variation explained by the principle coordinates is indicated at the axes.

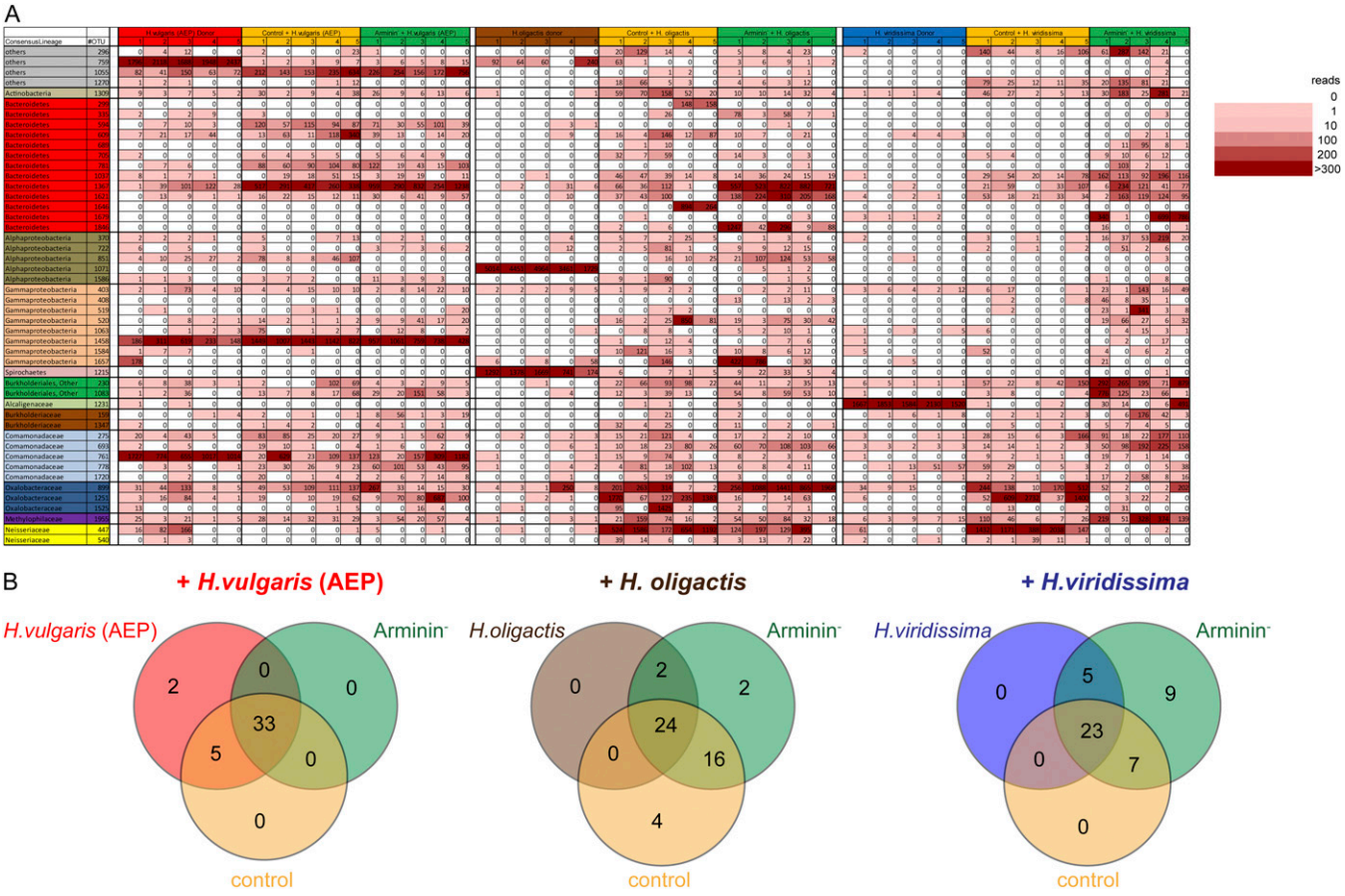

Fig. S7. (*A*) Heat-map of representative operational taxonomic units (OTUs, 97%) and Venn diagrams showing the presence of bacteria in donor and recipient polyps. Numbers represent counts of sequences per sample. OTUs were filtered using a threshold of at least 100 reads in one of the three experiments [re-colonization with *H. vulgaris* (AEP), *H. oligactis* (H.oli), or *H. viridissima* (H.vir)]. The remaining 48 OTUs are representing all bacterial groups shown in Fig. 6. (*B*) Venn diagrams showing the presence of bacteria between the donor species, control (yellow) and Arminin$^-$ (green) polyps. Note the significant overlap of donor species and the two recolonized groups (AEP recolonization: 33; H.oli recolonization: 24; and H.vir recolonization: 23).

Table S1. Tissue of Arminin$^-$ polyps shows a reduced antimicrobial activity against *Escherichia coli* DH5α

		MIC (μg/mL)	
Biological replicate	Date of extraction	Control	Arminin$^-$
#1	August 2012	1.563	3.125
#2	October 2012	0.781	1.563
#3	January 2013	3.125	6.250
Mean		1.823	3.646
RDA		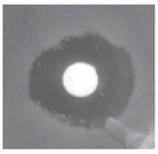	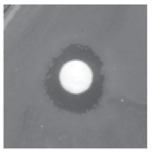

Small charged peptides were extracted from 1,000 polyps each as previously described (1). Antimicrobial activity was determined by minimal inhibitory concentration (MIC) assay, as well as radial diffusion assay (RDA) against *E. coli* DH5α. Three biological replicates were performed with peptide extractions conducted at different timepoints. MIC values are represented as mean of three biological replicates.

1. Augustin R, Siebert S, Bosch TC (2009) Identification of a kazal-type serine protease inhibitor with potent anti-staphylococcal activity as part of *Hydra*'s innate immune system. *Dev Comp Immunol* 33(7):830–837.

Table S2. Statistical tests comparing control and Arminin^{-} polyps recolonized by different bacterial communities

		Anosim		Adonis	
Strain	Metric	*R*	*P* value	R^2	*P* value
+ H.AEP	Weighted Unifrac	0.15	0.141	0.16	0.211
	Unweighted Unifrac	−0.03	0.575	0.11	0.412
	Bray–Curtis	0.24	0.042*	0.21	0.051
	Jensen–Shannon	0.24	0.051	0.26	0.028*
+ H.oli	Weighted Unifrac	0.62	0.007**	0.39	0.010**
	Unweighted Unifrac	0.13	0.155	0.13	0.241
	Bray–Curtis	0.84	0.010*	0.43	0.013*
	Jensen–Shannon	0.80	0.011*	0.52	0.011*
+ H.vir	Weighted Unifrac	0.82	0.008**	0.56	0.008**
	Unweighted Unifrac	0.47	0.040*	0.21	0.038*
	Bray–Curtis	0.90	0.005**	0.43	0.004**
	Jensen–Shannon	0.98	0.008**	0.60	0.011*

+H.AEP, *H. vulgaris* (AEP); +H.oli, *H. oligactis*; +H.vir, *H. viridissima*.
*$P < 0.05$, **$P < 0.01$, ***$P < 0.001$.